Journal of Environmental Chemical Engineering 9 (2021) 106794

Contents lists available at ScienceDirect

Journal of Environmental Chemical Engineering

journal homepage: www.elsevier.com/locate/jece

Health risk assessment of potentially toxic elements in the dry deposition fraction of settleable particulate matter in urban and suburban locations in the city of Gijón, Spain

Rosa Lara [a], Beatriz Suárez-Peña [b], Laura Megido [a,*], Luis Negral [c], Jesús Rodríguez-Iglesias [a], Yolanda Fernández-Nava [a], Leonor Castrillón [a]

[a] Department of Chemical and Environmental Engineering, Polytechnic School of Engineering, Gijón Campus, University of Oviedo, 33203 Gijón, Spain
[b] Department of Materials Science and Metallurgical Engineering, Polytechnic School of Engineering, Gijón Campus, University of Oviedo, 33203 Gijón, Spain
[c] Department of Chemical and Environmental Engineering, Technical University of Cartagena, Cartagena, Spain

ARTICLE INFO

Keywords:
Atmospheric settleable particles
Dustfall
Children's exposure
Heavy metal
Human health hazard

ABSTRACT

This study investigates the human health risk of Al, As, Fe, Mn, Ni, Pb, Sb and Sr in the dry deposition fraction of settleable particulate matter (DSPM). Sixty samples were collected at an industrial suburban site ('EMA') and a waterfront urban site ('Naval') in Gijón, a coastal city in northern Spain. Up to 4898.4 mg m^{-2} d^{-1} were measured at the station closer to industrial activity. The levels of the eight elements were greater at this site. Fe and Al were the major constituents, comprising up to 50% of DSPM.

The human health risk posed by DSPM was assessed using a U.S.EPA methodology. The level of exposure to the metals/metalloids in this atmospheric pollutant was studied via ingestion, inhalation, and dermal contact. The results showed that ingestion was the main exposure pathway for the residents at the two locations, followed by dermal contact and inhalation. For adults, the non-carcinogenic hazard indexes and the carcinogenic risk levels of the eight elements were within the acceptable levels (1 and 10^{-5}, respectively). Nevertheless, in the case of children, the non-carcinogenic hazard indexes of Fe and Pb as well as the carcinogenic risk level of As via ingestion were higher than those thresholds.

Despite its importance, little research has focused on assessing the human risk posed by metals/metalloids in DSPM. Although there are uncertainties regarding the exposure factors and toxicity values, the outcomes of this study provide useful knowledge for regulatory authorities to establish appropriate mitigation measures to reduce DSPM emissions in urban and suburban environments.

1. Introduction

Particulate matter may originate from natural sources (soil erosion, sandstorms, etc.), but may also be a consequence of endlessly expanding anthropogenic activities (industry, vehicle and road wear, construction and demolition, for example). These particles may contain a wide range of toxic substances, such as heavy metals, polycyclic aromatic hydrocarbons, NH_4^+, SO_4^{2-} and NO_3^-.

Both short-term and long-term effects on human health have been linked to atmospheric dust. Furthermore, substantial epidemiologic evidence supports its relationship with increased daily morbidity and mortality [13]. Some sectors of the population are likely to be more exposed and/or vulnerable to this air pollutant depending on their lifestyle, previous health conditions or age. Children, for instance, may have respiratory, immune, reproductive, central nervous and digestive systems that have still not fully developed and thus, the same environmental conditions might have a greater impact on them than on adults [33].

The European legislation on ambient air quality (Directive 2008/50/EC) only establishes a limit value for the finer fractions of atmospheric dust (PM2.5 and PM10). Coarse particles are much less likely to be inhaled, through the mouth and nose, than smaller particles. However, ingestion and dermal contact are also important exposure routes to this atmospheric pollutant [35] and the possible effects on human health may not be insignificant. Indeed, Sobhanardakani [40] found that ingestion of atmospheric dust was the main exposure route to heavy

* Corresponding author.
E-mail address: megidolaura@uniovi.es (L. Megido).

https://doi.org/10.1016/j.jece.2021.106794
Received 9 November 2021; Accepted 10 November 2021
Available online 15 November 2021

metals in Hamedan, a city in Iran.

Heavy metals are non-biodegradable and environmentally persistent substances [36,41]. They can accumulate in several human organs (kidney, liver, lungs and brain, among others) leading to severe diseases (cancer, dementia, organ dysfunction, haemorrhage, paralyses, bronchitis and more) [3]. The International Agency for Research on Cancer (IARC) has classified more than a thousand agents according to the available evidence that supports their carcinogenicity for humans, including metals/metalloids. For example, aluminium production, arsenic and inorganic arsenic compounds, iron and steel founding (occupational exposure during), and nickel compounds fall into Group-1, which comprises agents considered to be 'carcinogenic to humans'. Antimony trioxide, metallic nickel and lead are categorized as falling within Group-2B, i.e., possibly carcinogenic to humans. This group-based classification is frequently updated based on new evidence about the included agents and/or to add new agents. In 2006, for instance, inorganic and organic lead compounds were incorporated into Groups 2A ('probably carcinogenic to humans') and 3 ('not classifiable as to its carcinogenicity to humans'), respectively. Interestingly, in 2016, outdoor air pollution and particulate matter in outdoor air pollution were both added to Group 1 [16].

Dry deposition is one of the main routes by which heavy metals are transferred into the topsoil in urban areas [51]. Despite its importance and as noted by Sobhanardakani [42], few studies in the literature assess the human risk posed by heavy metals in the dry fraction of settleable particle matter (DSPM).

On a very preliminary risk assessment, Negral et al. [31] found that DSPM might be potentially dangerous to the health of residents in Gijón, an industrial city on the north coast of Spain. That study was mainly focused on the levels, chemical composition, and morphology of settleable particle matter. The human health risk assessment considered only two exposure pathways: ingestion and dermal contact. The risk indicators of As, Sb and Pb in DSPM stood out from the rest of the chemical elements analysed, due to their high values. In view of these results, the aim of the present study is to deepen the understanding of the possible hazards posed by metals/metalloids in DSPM in Gijón. To do so, the health risks of Al, As, Fe, Mn, Ni, Pb, Sb and Sr were assessed and compared at an industrial suburban site and an urban site.

The eight metals/metalloids selected for this study may occur in urban and suburban settings and have a toxicological profile [7]. Al is a recognized neurotoxin that hinders more than 200 biological functions and may produce adverse effects in plants, animals, and humans [19]. As may increase mortality from skin cancer, liver cancer, prostate cancer, etc. [14]. Fe overload has been linked to failure of heart, liver and pancreas, among other organs [34]. Mn toxicity mainly affects the central nervous system [24]. Ni has been associated with allergy, cardiovascular and kidney diseases, lung fibrosis, lung, and nasal cancer [8]. Pb can cause adverse effects on the nervous, endocrine, circulatory and renal systems [52]. All Sb and Sb compounds are toxic to the human body, those of Sb^{3+} having much higher toxicity than Sb^{5+} compounds [22]. Sb has been linked to effects on the heart after long-term exposure and tends to accumulate in the thyroid, adrenals, liver, and kidney [43]. Lastly, when exposed to excessive stable Sr, which is present naturally in minerals, children are more vulnerable than adults and problems of bone growth may appear if there are other deficiencies (Ca, protein…) [2].

The health risk assessment carried out in the present study was based on the guidelines defined by the U.S. Environmental Protection Agency (U.S.EPA). Ingestion, inhalation, and dermal contact were the routes of exposure evaluated. The results of this research led to the identification of the metals/metalloids of the highest concern for children and adults exposed to DSPM in Gijón. The identification of cancer and non-cancer risks posed by this air pollutant is necessary and useful in order to take action towards better protection of human health in urban and suburban settings.

2. Materials and methods

2.1. Sampling locations

The study area was in Gijón, an industrial region on the shore of the Cantabrian Sea (northern Spain). Numerous industries are located mainly in the western part of the urban area, as indicated in Fig. 1. The municipal area of Gijón has a population density of 1492 inhabitants km^{-2} (271717 inhabitants) [17].

Two sampling stations, separated less than 3 km from each other (Fig. 1), were used: 'EMA' (43°32'24.2"N 5°43'1.3"W), an industrial suburban station located 60 m above mean sea level in Veriña, a neighbourhood close to the industrial area; and 'Naval' (43°32'28.3"N 5°40'48.6"W), an urban station at 3 m above sea level in the Natahoyo district.

2.2. Sampling

24-h DSPM samples were simultaneously collected from December 2019 to June 2020 at the EMA and Naval stations using 1 m^2 square methacrylate trays (Fig. S1), resulting in thirty DSPM samples at each location. Each sample was collected on days without rainfall between 4 p.m. on one day and 4 p.m. on the next one. Then, it was swept off the tray with a rubber scraper and subsequently placed in a PET container. The accumulated mass (mg m^{-2} d^{-1}) was determined gravimetrically.

Furthermore, 24 h samples were also collected on 1 cm^2 silicon crystals, which were attached to a metal support by a double-sided adhesive film. These samples were analysed by scanning electron microscopy (SEM).

2.3. Measurement of metals/metalloids

Al, As, Fe, Mn, Ni, Pb, Sb and Sr were measured in the DSPM samples, after chemical digestion with HF, HNO_3 and $HClO_4$ [26]. As a quality control, the same procedure was applied to the Standard Reference Material®1648a from the NIST [31]. The analysis was carried out using inductively coupled plasma mass spectrometry (ICP-MS Agilent 7500). Analytical errors were mostly kept $< 10\%$ (see Supplementary Material), in line with previous studies [25,31].

2.4. SEM analysis

DSPM samples collected on silicon crystals were covered with gold using a cathodic pulverization Bal-Tec SCD 005 sputtering device (40 mA, 360 s sputtering). Then, microstructural observation was carried out by means of a JEOL JSM 5600 SEM (JEOL Ltd., Tokyo, Japan). The accelerating voltage used was 20 kV, the working distance 15 mm and the beam spot size was 3.

2.5. Statistical analysis

The normality of the dataset was studied using the Shapiro-Wilk normality test ($p < 0.01$). Given that the data did not follow a normal distribution, the relationship between variables was analysed by the Spearman correlation test. The Duncan's multiple range test was used to compare pairs of mean levels obtained at the two sampling sites. The statistical software used was R4.0.4.

2.6. Risk assessment model: description and assumptions

The model used to estimate the potential exposure to Al, As, Fe, Mn, Ni, Pb, Sb and Sr in DSPM and their human health effects was developed by the U.S.EPA. The relationship between human exposure, dose and adverse effects is studied in the risk assessment [39].

In the present work, the potentially exposed population considered was composed of the residents at the two studied locations. The target

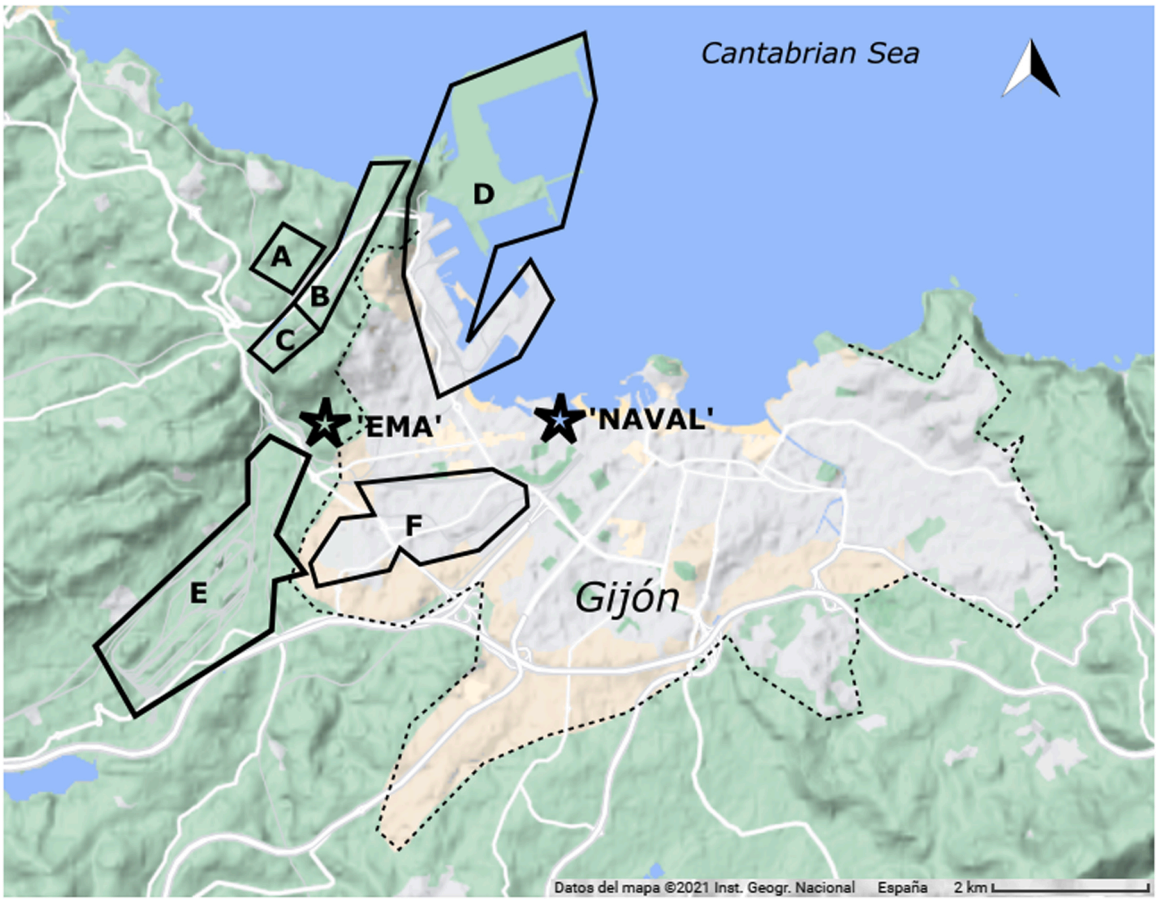

Fig. 1. Location of the sampling stations, named 'EMA' and 'Naval', in the city of Gijón and the main industries in the surroundings: A) cement plant; B) coal stockyard; C) coal-fired power plant; D) port of Gijón ('El Musel'); E) steelworks; and F) industrial estate. (Image created using Google Maps Terrain and Inkscape 0.92.4).

subjects were divided in two groups: children (<6 years) and adults (>20 years) [49]. The biometric and exposure parameters of the residents were assumed to be similar to those of the U.S. residents. The routes of exposure to the eight aforementioned elements were: direct ingestion of particles, inhalation and dermal absorption of elements in particles adhering to exposed skin. The dose received by these pathways was calculated by the following expressions [46,47]:

$$D_{ing} = C \cdot \frac{IngR \cdot EF \cdot ED}{BW \cdot AT} \cdot CF \quad (1)$$

$$D_{inh} = C \cdot \frac{InhR \cdot EF \cdot ED}{PEF \cdot BW \cdot AT} \quad (2)$$

$$D_{der} = C \cdot \frac{SA \cdot SL \cdot ABS \cdot EF \cdot ED}{BW \cdot AT} \cdot CF \quad (3)$$

where,

D (mg kg^{-1} d^{-1}): dose of DSPM received through ingestion (D_{ing}), inhalation (D_{inh}) and dermal contact (D_{der}); C (mg kg^{-1}): concentration of potentially toxic elements in DSPM ('exposure point concentration'); IngR: ingestion rate (in this study, it was assumed to be the same as that for soil, i.e., 200 mg d^{-1} for children and 100 mg d^{-1} for adults); EF: exposure frequency, 350 d y^{-1}; ED: exposure duration, 6 years for children and 20 years for adults; BW: average body weight, 15 kg for children and 80 kg for adults; AT: average time, (ED·365) d for non-carcinogens and (70·365) d for carcinogens; CF: conversion factor, 10^{-6} kg mg^{-1} [48]; InhR: inhalation rate (7.6 m^3 d^{-1} for children and 20 m^3 d^{-1} for adults) [40,42]; PEF: particle emission factor ($1.36 \cdot 10^9$ m^3 kg^{-1}) [50]; SA: exposed skin area, 2373 cm^2 for children and 6032 cm^2 for adults; SL: skin adherence factor, 0.2 mg cm^{-2} for children and 0.07 mg cm^{-2} for adults; ABS: dermal absorption factor (unitless), 0.001 for all elements except arsenic, which was 0.03 [50]. The values of these parameters were taken from the Standard Default Exposure Factors of USEPA [49].

The 'exposure concentration point' and the exposure-related parameters assumed a 'reasonable maximum exposure', i.e., the maximum exposure that is reasonably expected to occur at a particular location. In this study, C was the upper limit of the 95% confidence interval (95% UCL) for the concentrations of an element found in the DSPM samples [44]. These 95% UCL were calculated with the software R4.0.4.

In accordance with [44,48], non-cancer risk was evaluated by means of the hazard quotient (HQ). HQ was the result of dividing the calculated dose for each element and route of exposure (Eqs.(1)–(3)) by the corresponding reference dose, RfD (Table 1). Moreover, the sum of the HQs calculated for each element for the three exposure pathways gives the hazard index (HI), which is the aggregate non-cancer risk [44].

Additionally, cancer risk (CR) is the "incremental probability of an individual's developing cancer over a lifetime as a result of exposure to a potential carcinogen" [45]. Arsenic and nickel are the only elements considered in this study that has a potential carcinogenic effect [50]. Their CR were calculated by multiplying the doses (Eqs.(1)–(3)) by the corresponding slope factor, Sf (Table 1). The overall CR for children and adults (RISK) was calculated by adding the individual risks of both routes of exposure [44].

Table 1
Concentration term (C (95% UCL), in mg/kg), reference doses (RfD, in mg kg^{-1} d^{-1}) and slope factor (Sf, in kg d mg^{-1}) from [50], except for Pb [54]. Results of the HQ (unitless), HI (unitless), CR (unitless) and RISK (unitless) for elements in DSPM via ingestion (ing), inhalation (inh) and dermal contact (der) at the EMA and Naval stations for children and adults (HQ>1, HI>1, CR>1.00E-05 and RISK>1.00E-05 are highlighted in bold).

Element	C	RfD_{ing}	RfD_{inh}	RfD_{der}	Sf_{ing}	Sf_{inh}	Sf_{der}	HQ_{ing}		HQ_{inh}		HQ_{der}		HI		CR_{ing}		CR_{inh}		CR_{der}		RISK	
								Children	Adults	Children	Adults	Children	Adults	Children	Adults	Children	Adults	Children	Adults	Children	Adults	Children	Adults
EMA station																							
Al	8137.42	1.00E+ 00	1.40E-03	1.00E-01				1.04E-01	9.75E-03	2.08E-03	1.02E-03	2.47E-03	4.12E-04	1.09E-01	1.12E-02								
As	7.25	3.00E-04	4.30E-06	1.20E-04	1.50E+ 00	1.51E+ 01	3.70E+ 00	3.09E-01	2.90E-02	6.05E-04	2.97E-04	5.50E-02	9.17E-03	3.65E-01	3.84E-02	**1.19E-05**	3.73E-06	3.37E-09	5.52E-09	2.09E-06	1.16E-06	**1.40E-05**	4.89E-06
Fe	415483.95	7.00E-01	2.20E-04	7.00E-02				**7.59E+ 00**	7.11E-01	6.77E-01	3.33E-01	1.80E-01	3.00E-02	**8.44E+ 00**	**1.07E+ 00**								
Mn	1428.19	4.60E-02	1.43E-05	1.80E-03				3.97E-01	3.72E-02	3.58E-02	1.76E-02	2.41E-02	4.02E-03	4.57E-01	5.88E-02								
Ni	70.78	2.00E-02	2.06E-02	5.40E-03		8.40E-01		4.52E-02	4.24E-03	1.23E-06	6.06E-07	3.98E-04	6.63E-05	4.56E-02	4.31E-03			1.83E-09	2.99E-09			1.83E-09	2.99E-09
Pb	35.28	3.50E-03	3.52E-03	5.30E-04				1.29E-01	1.21E-02	3.59E-06	1.77E-06	2.02E-03	3.37E-04	1.31E-01	1.24E-02								
Sb	2.73	4.00E-04	4.00E-04	8.00E-06				8.72E-02	8.18E-03	2.45E-06	1.20E-06	1.04E-02	1.73E-03	9.76E-02	9.91E-03								
Sr	232.07	6.00E-01		1.20E-01				4.94E-03	4.63E-04			5.87E-05	9.79E-06	5.00E-03	4.73E-04								
Naval station																							
Al	10664.00	1.00E+ 00	1.40E-03	1.00E-01				1.36E-01	1.28E-02	2.73E-03	1.34E-03	3.24E-03	5.40E-04	1.42E-01	1.47E-02								
As	8.31	3.00E-04	4.30E-06	1.20E-04	1.50E+ 00	1.51E+ 01	3.70E+ 00	3.54E-01	3.32E-02	6.93E-04	3.41E-04	6.30E-02	1.05E-02	4.18E-01	4.40E-02	**1.37E-05**	4.27E-06	3.86E-09	6.32E-09	2.40E-06	1.33E-06	**1.61E-05**	5.60E-06
Fe	109660.97	7.00E-01	2.20E-04	7.00E-02				**2.00E+ 00**	1.88E-01	1.79E-01	8.79E-02	4.75E-02	7.93E-03	**2.23E+ 00**	2.83E-01								
Mn	1495.71	4.60E-02	1.43E-05	1.80E-03				4.16E-01	3.90E-02	3.75E-02	1.84E-02	2.52E-02	4.21E-03	4.78E-01	6.16E-02								
Ni	45.26	2.00E-02	2.06E-02	5.40E-03		8.40E-01		2.89E-02	2.71E-03	7.88E-07	3.87E-07	2.54E-04	4.24E-05	2.92E-02	2.75E-03			1.17E-09	1.91E-09			1.17E-09	1.91E-09
Pb	1043.48	3.50E-03	3.52E-03	5.30E-04				**3.81E+ 00**	3.57E-01	1.06E-04	5.23E-05	5.97E-02	9.96E-03	**3.87E+ 00**	3.67E-01								
Sb	8.19	4.00E-04	4.00E-04	8.00E-06				2.62E-01	2.45E-02	7.34E-06	3.61E-06	3.11E-02	5.18E-03	2.93E-01	2.97E-02								
Sr	377.95	6.00E-01		1.20E-01				8.05E-03	7.55E-04			9.56E-05	1.59E-05	8.15E-03	7.71E-04								

3. Results and discussion

3.1. Levels of dry deposition

The values of DSPM collected at two sampling stations are shown in Fig. S2 and Table S1. In general, the amount of dry matter collected was greater at the location closer to the industrial zone (EMA station) throughout the sampling period, and values up to 4898.4 mg m^{-2} d^{-1} were measured (1529.1 ± 1543.7 mg m^{-2} d^{-1}, n = 30). At the Naval station, the highest value registered was 69.2 mg m^{-2} d^{-1} (25.2 ± 18.4 mg m^{-2} d^{-1}, n = 30). The Duncan's multiple range test revealed that these DSPM means were significantly different (p-value<0.01). This was to be expected as the fraction of atmospheric particles collected is mainly composed of coarse particles, which generally settle near their source. The residence time of particles in the atmosphere (1–6 days) is function of their dry Lagrangian path and mainly depends on their size and chemistry. Due to their size, coarse particles usually remain in the atmosphere for only short periods of time, as they are easily removed by dry deposition [56], which implies that the travel distance is shorter than for fine particles.

It is important to note that 67% of the DSPM samples at the EMA station exceeded the value of 300 mg m^{-2} d^{-1}, which was the limit value established in Spain until 2002 for settleable particulate matter (there understood as the sum of dry deposition and wet deposition). The variability observed in the DSPM levels may be explained by a complex mixture of factors, including changes in the fluxes generated by the emission sources and meteorological conditions (e.g., rain during the transport to the site, rain intensity on the previous days, atmospheric stability, wind speed and wind direction) [1]. Furthermore, a difference was detected at both locations in the levels of DSPM recorded after lockdown measures were introduced in mid-March 2020 due to the coronavirus SARS-CoV-2 (Table S1). Particularly, at the EMA station, the mean levels recorded decreased from 2375.3 ± 1331.6 mg m^{-2} d^{-1} (n = 19) to 67.6 ± 95.5 mg m^{-2} d^{-1} (n = 11). The reduction in the industrial activity and road traffic during the lockdown might explain these values. Nonetheless, an in-depth study is needed to assess whether these changes are significant and rule out the influence of meteorological variability. Negral et al. [31] found that DSPM ranged from 8.6 to 830.3 mg m^{-2} d^{-1} in western districts of Gijón from April to May in 2018. Santos et al. [37] studied SPM in eight locations in the Metropolitan Region of Vitoria (Brazil) and found levels ranging from 2 to 20 g m^{-2} $30d^{-1}$ (i.e., 67–667 mg m^{-2} d^{-1}). Steel and iron ore pelletizing industries were identified as the main contributors to DSPM in the area, on account of its composition (elemental and carbon, Fe, Al, and Si).

3.2. Metals/metalloids

Following the trend observed in the DSPM levels, the concentrations of all elements measured in the DSPM samples showed a spatial variability, with higher values at the EMA station than at the Naval station. Moreover, some of them showed high dispersion (Fig. 2, Table S2). The Duncan's multiple range test showed that the mean levels obtained at each site were significantly different (p-value<0.01; except for Pb: p-value<0.05).

3.2.1. Major elements

Regardless of the sampling station, Fe reached the highest values, followed by Al: 656.8 ± 678.6 mg Fe·m^{-2}·d^{-1} and 11.1 ± 10.5 mg Al·m^{-2}·d^{-1} were measured at the EMA station, and 2.7 ± 4.2 mg Fe·m^{-2}·d^{-1} and 0.2 ± 0.2 mg Al·m^{-2}·d^{-1} at the Naval station. Indeed, Fe and Al alone represented, respectively, 37.3 ± 11.4% and 0.8 ± 0.1% of DSPM at the EMA station and 8.3 ± 7.3% and 0.9 ± 0.5% at the Naval station.

These two elements are among the most abundant in the Earth's upper crust composition and specifically in samples of soil and sediments in the surroundings of the sampling stations which are characterized by the presence of limestones, dolomites, black and wine-coloured clays, red sandstones, and conglomerates [18]. Besides erosion of earthen materials and windblown transport, industries and other anthropogenic activities (e.g., traffic movement may cause the resuspension of particles) may greatly contribute to the quantity of particles in the atmosphere [27].

Although regarded as a crustal element, Al particles are also generated in different industrial processes, such as the aluminium industry, sintering processes, etc. The highest levels of Al in DSPM were 33.4 and 0.9 mg m^{-2} d^{-1} at the EMA and Naval stations, respectively. The lowest values were found after the start of the lockdown, as seen in DSPM levels (at the EMA station: 0.6 ± 0.9 mg m^{-2} d^{-1}, n = 11; at the Naval station: 0.1 ± 0.2 mg m^{-2} d^{-1}, n = 11). Likewise, the lowest values of Fe were found after the start of the lockdown: 21.0 ± 32.2 (n = 11) and 0.4 ± 0.3 mg m^{-2} d^{-1} (n = 11) at the EMA and Naval stations, respectively. Nonetheless, Fe reached a maximum of 2473.4 mg m^{-2} d^{-1} at the former, representing 50.5% of the DSPM level determined that day. A value of 21.3 mg m^{-2} d^{-1} was the maximum detected at the Naval station during the sampling period.

Al and Fe showed a stronger correlation between each other (ρ = 0.99, p-value<0.01) at the sampling station closest to the industrial area than at the one furthest away (ρ = 0.87, p-value<0.01). Both Al and Fe particles may have originated in the nearby steel plant. Iron is one of the major elements found in dust from integrated iron and steel

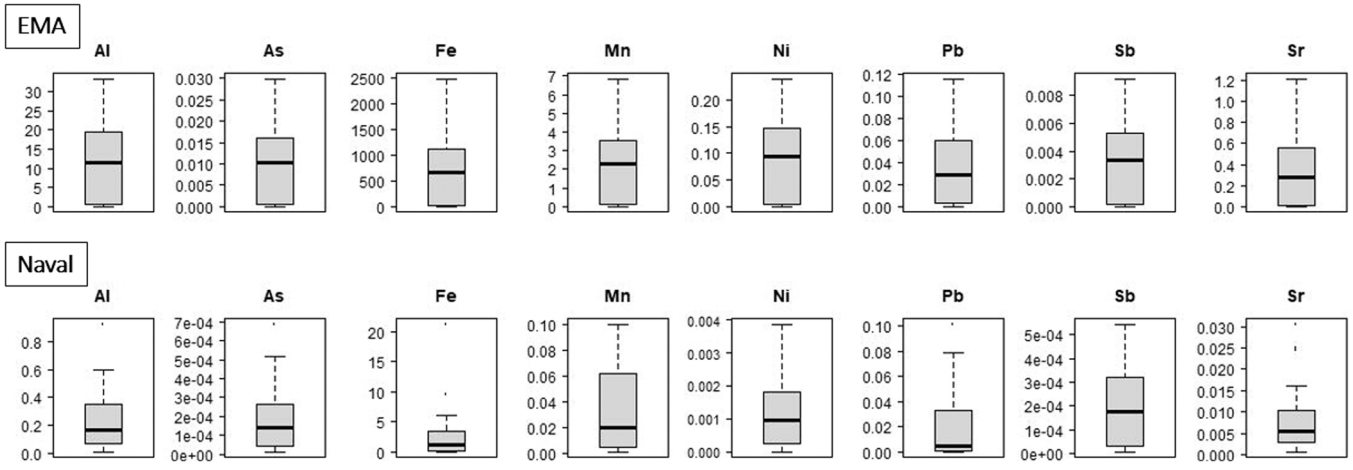

Fig. 2. Box plots of the levels of eight chemical elements, expressed in mg m^{-2} d^{-1}, in DSPM samples collected at the EMA and Naval stations (n = 30 samples at each station) from December 2019 to June 2020 (outliers being values below Q1–1.5·IQR or above Q3 +1.5·IQR, where IQR is the interquartile range).

facilities. Moreno et al. [30] determined that > 30% of the air particles in Port Talbot (United Kingdom) were iron spherules; their sampling location was 800 m away from a steel plant. Furthermore, these facilities generate fugitive dust emissions, which contain high amounts of heavy metals that are embedded in the particles [12]. These researchers found that Fe, Ca, Al, and Mg were the major elements in particles from sintering, blast furnace, steelmaking, and desulfurization slag processes; Zn and Pb were also associated with the steel industry. In the present study, the different processes in the steelworks are located very close to each other within the industrial facility, which makes it difficult to distinguish between them in the DSPM samples by considering meteorological parameters like predominant wind direction on the sampling day, for instance. Additionally, other external sources, like resuspension of previously deposited particles, may have contributed to DSPM.

3.2.2. Minor elements

The other elements that were analysed in DSPM samples were present at lower levels (Fig. 2; Table S2) and following the order Mn>Sr>Ni>Pb>As>Sb at the EMA location, whereas at the Naval station the sequence was: Mn>Pb>Sr>Ni>Sb>As.

At the EMA station, up to 6.9 mg m^{-2} d^{-1} of Mn were measured during the sampling period (2.1 ± 2.0 mg m^{-2} d^{-1}, on average), whereas at the Naval station, the highest value recorded was 0.1 mg m^{-2} d^{-1}. Metallurgical activities mainly released Mn in oxide form; the oxidation state has an influence on toxicity mechanisms. In fact, Mn^{3+} and Mn^{2+} have both been proved to be neurotoxic [55]. Interestingly, the levels of Mn determined in DSPM samples taken on the same day at the two sampling stations showed certain correlation between each other ($\rho = 0.64$, p-value<0.01). This may point to a common emission source contributing to Mn in DSPM at both locations. The same was observed with the levels of Fe determined at the two sampling stations ($\rho = 0.65$, p-value<0.01). Like Fe, Mn is a characteristic tracer of the steelmaking industry and > 10 μg Mn/m^3 may be found in the surroundings of iron, steel, or alloy facilities [9]. Fe, Mn, Pb and Zn in PM10 were traced back to the steelworks in a source apportionment study carried out during 2013–2014 at a suburban site in the east of Gijón [26]. That study also pointed to combustion sources being the responsible for Ni, Co, K, and organic matter. Ni and Co are usually considered as tracers of industrial combustion (petroleum and coal combustion and oil burning, among others).

In the present study, all elements found in DSPM samples showed $\rho > 0.90$ (p-value<0.01) between each other at the EMA station, except for Ni–Pb ($\rho = 0.85$, p-value<0.01). By contrast, at the Naval station only Al–As, Al–Mn, Al–Ni, Al–Sr, As-Mn and Fe-Mn presented such high correlation. Nonetheless, the rest of the elements were linked to some extent with each other ($\rho > 0.60$, p-value<0.01).

Apart from the previously mentioned case of Fe and Mn, the levels of certain elements recorded at both sampling sites on the same day showed some correlation. This was the case of Sb, Ni and As ($\rho = 0.70$, 0.57, 0.52, respectively; p-value<0.01). However, for the rest of the elements under study $\rho < 0.50$ and/or p-value ≥ 0.01, which may be related to different sources contributing at each sampling location to the accumulation of these elements, for instance. Furthermore, the size, morphology (i.e., single particles or agglomerates) and/or density of the particles may affect their movement in the atmosphere. Thus, large and/or heavy particles of an element may reach the EMA station but not the Naval station, also depending on meteorological conditions.

The spatial variability seen in DSPM, Al and Fe was also observed with five out of the six minor elements (Table S2). For instance, a mean value of 9.7 ± 9.0 μg m^{-2} d^{-1} of As was measured at the EMA station during the whole sampling period, with a corresponding value of only 0.2 ± 0.2 μg m^{-2} d^{-1} at the Naval station, levels reaching maximums of 29.9 and 0.7 μg m^{-2} d^{-1}, respectively. However, Pb constituted an exception to that spatial variability, as the levels determined were in the same order of magnitude at both locations: 35.3 ± 34.7 and 19.2 ± 26.4 μg m^{-2} d^{-1} at the EMA and Naval stations, respectively. The maximum values were also quite similar (116.5 and 101.3 μg m^{-2} d^{-1}, respectively). Nevertheless, Pb comprised 0.001–0.008% of DSPM at the EMA station, but 0.004–0.400% at the Naval station. At the latter location, although Pb showed $\rho > 0.70$ with all the other elements studied in DSPM, its highest correlation was with Mn ($\rho = 0.83$, p-value<0.01), followed by As ($\rho = 0.78$, p-value<0.01). The metallurgic industry and coal combustion are among the major man-made sources of As and Pb released into the environment [57,58]. Based on concentrations measured in PM10, the emissions of these two elements from anthropogenic sources decreased by 35% and 68%, respectively, in EU-28 from 2000 to 2018 [7].

Sb is an element that is a common component of coal and petroleum. Thus, fossil fuel burning, and industrial emissions are important sources [10]. Sb was collected within the ranges 0.02–9.2 and 0.01–0.6 μg m^{-2} d^{-1} at the EMA and Naval stations, respectively. Fossil fuel combustion and high temperature metallurgical operations are also important sources of Ni [21]. Indeed, these authors cannot discard the possibility that Ni levels may be affected by the activities of ships in locations close to port. In the present study, at the station closest to the port, Ni was highly linked to Al ($\rho = 0.93$, p-value<0.01) and the highest value detected was 3.9 $\mu g \cdot m^{-2} \cdot d^{-1}$. However, at the station closest to the industrial area, mean Ni levels were 84.9 $\mu g \cdot m^{-2} \cdot d^{-1}$ and the maximum was 239.5 $\mu g \cdot m^{-2} \cdot d^{-1}$. The nearby industries may make the largest contribution to Ni in DSPM, given that it is used in several metallurgical processes (alloy production, electroplating…).

Likewise, the levels of Sr were greater at the EMA station (336.59 ± 341.6 μg m^{-2} d^{-1}) than at the Naval station (7.99 ± 7.49 μg m^{-2} d^{-1}), the maximum values being 1214.9 and 30.6 μg m^{-2} d^{-1}, respectively. The Sr compounds in the atmospheric dust may be emitted during coal and oil combustion.

3.3. Health risk assessment

Ingestion, inhalation, and dermal contact have been considered as the main routes of exposure to metals/metalloids through DSPM. Thus, HQ and CR values obtained for each of the analysed elements are shown in Table 1. As, Fe and Pb were the elements of major concern in terms of human health at the two urban/suburban locations under study.

The results of the non-carcinogenic risk assessment indicate that the ingestion route would pose the highest risk to Al, As, Fe, Mn, Ni, Pb, Sb and Sr in DSPM, for both children and adults, regardless of the location, followed by dermal contact and inhalation. These results agree with those found by Weerasundara et al. [53], who concluded that the exposure routes via ingestion and dermal contact are more important than inhalation in terms of human risk. Indeed, they found that HQ_{ing} of atmospheric dust accounted for 95% of the HI in Kandy, a city in Sri Lanka. Their results agreed with previous studies [6,23].

In the present study, regardless of the sampling station, HQ values were higher for children than for adults, by at least one order of magnitude in almost every element for the ingestion and dermal contact pathways. Indeed, for children at the EMA station, the HQ_{ing} for Fe ($HQ_{ing,Fe}$=7.59) exceeded the acceptable level (HQ≤1) and at the Naval station the same was true of Fe and Pb ($HQ_{ing,Fe}$=2; $HQ_{ing,Pb}$=3.81).

In the case of the inhalation route, the HQ_{inh} values were similar for both children and adults, varying between $3.87 \cdot 10^{-7}$ and $6.77 \cdot 10^{-1}$, depending on the element considered. All values were within acceptable levels. Nonetheless, it is important to point out that in the present study the calculations have been done considering that all particles could be inhaled, regardless of their size. However, the size of the particles influences their probability of being inhaled and deposited in the human respiratory tract. Models make it possible to estimate the fraction of inhaled and deposited particles according to the range of aerodynamic diameters, those above 10 μm being less likely to be inhaled and if so, to reach deeper regions in the human respiratory tract. Indeed, the finer particles within this fraction (PM2.5) have been associated with the greatest risks to human health [11,15,28].

The SEM images of DSPM samples (Fig. 3) show particles with a wide range of sizes. Some of them have maximum Feret diameters below 100 μm. These particles may be resuspended, facilitating their inhalation through the nose or mouth [20,29]. Particles larger than 100 μm are also observed in the micrographs. For these, the movement mechanisms would be saltation (i.e., bouncing near the air-surface interface) and/or surface creep (i.e., rolling along the surface) [4,38], which would make it more difficult for them to enter the human body through breathing. Therefore, the assumption that all particles in the DSPM samples can be inhaled may overestimate the health risk via inhalation.

HQ and HI values were similar at the two sampling stations and in general, greater for children than adults. The HI values of Fe obtained for children were 8.44 and 2.23 at the EMA and Naval stations, respectively; both HI values were above the acceptable threshold of 1. The HI of Pb also exceeded this value for children at the Naval station (HI_{Pb}=3.87). In the case of adults, only the HI of Fe at the EMA station exceeded the acceptable level (HI_{Fe}=1.07).

The cancer risk assessment revealed ingestion as the main exposure route. The CR values for As via ingestion were one order of magnitude higher for children than for adults, regardless of the location. However, the CR values for inhalation and dermal contact for both children and adults were of a similar order of magnitude.

The CR of As via ingestion for children ($1.19{\cdot}10^{-5}$ and $1.37{\cdot}10^{-5}$ at the EMA and Naval stations, respectively) were slightly above the acceptable level ($CR \leq 10^{-5}$). Thus, the RISK was also above $1{\cdot}10^{-5}$, suggesting that the cancer risk posed by As is not negligible to this sector of the residents at the two locations.

In the case of Ni, the CR_{inh} and RISK values were below the acceptable level at both sites.

The results of the human health risk assessment together with the high levels of DSPM reported at the station closer to the industrial facilities showed the importance of establishing measures to control this atmospheric pollutant and take action towards better protection of human health in urban and suburban settings.

It is important to acknowledge that these results should be interpreted with due caution as they are influenced by a level of uncertainty, linked to the exposure parameters and the toxicity values, among others, assumed in the risk assessment. Additionally, previous exposure of children and adults to toxic elements through dietary intake or by other routes may affect the overall risk [5,32].

4. Conclusions

Sixty 24-h DSPM samples were collected at an industrial suburban site and an urban site in Gijón (Spain). The levels registered were higher at the sampling station closer to the nearby steel plant. This spatial variability from the suburban to the urban site was also observed in Al, As, Fe, Mn, Ni, Sb and Sr; the only exception was Pb. The human health risk posed by these eight elements present in DSPM was assessed via ingestion, inhalation, and dermal contact. Regardless of the location, ingestion implied the greatest potential cancer and non-cancer risks, followed by dermal contact and inhalation. The non-cancer indicators showed greater values for children than adults. Indeed, in the case of children, the HQ_{ing} and HI of Fe exceeded the acceptable level at the EMA station and the HQ_{ing} and HI of Fe and Pb at the Naval station too. For adults, the threshold was only surpassed by the HI of Fe at the EMA station. Furthermore, the CR_{ing} and RISK of As were above the acceptable level for children, regardless of the location. In the case of Ni, cancer risk indexes were within acceptable limits for children and adults. These results highlight the need for establishing mitigation and control measures to decrease DSPM levels in urban/suburban locations.

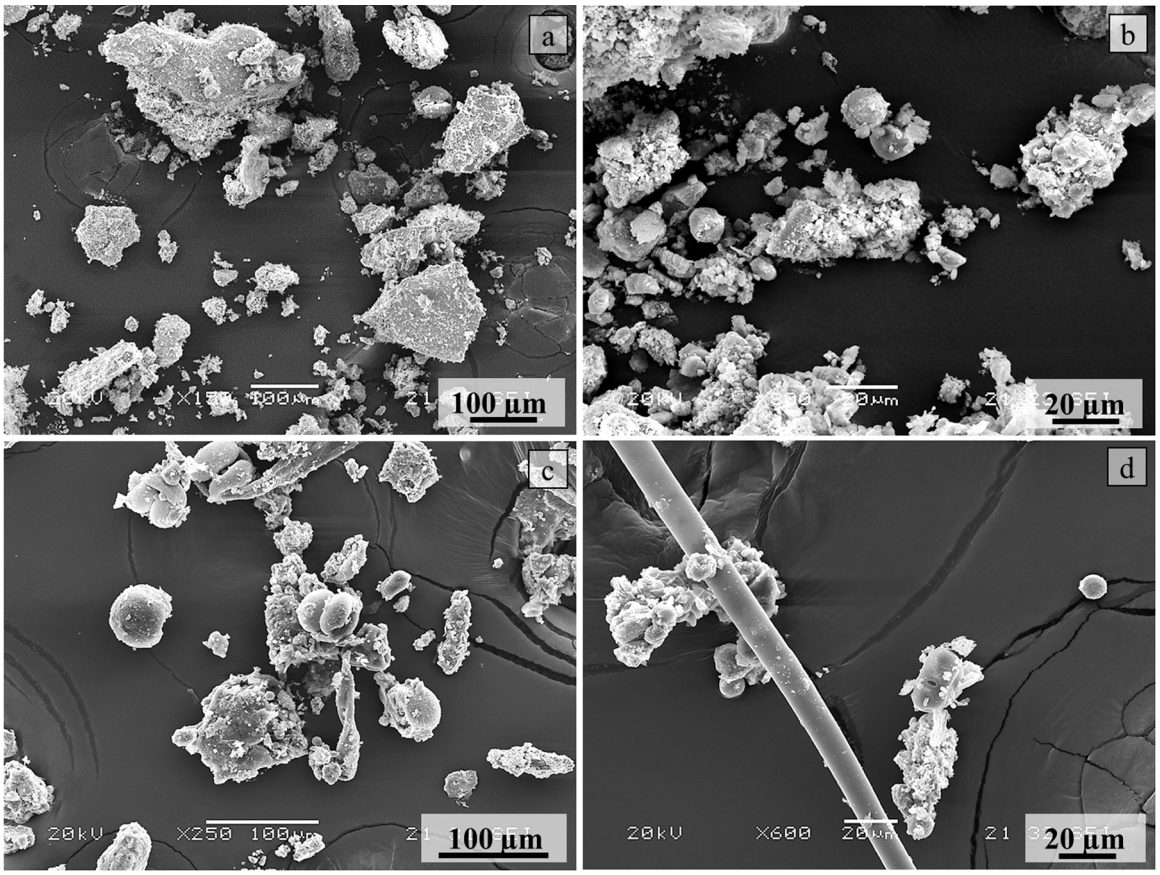

Fig. 3. SEM micrographs showing the heterogeneity of particle sizes in DSPM samples collected at the EMA (a-b) and Naval (c-d) locations.

Declaration of Competing Interest

The authors declare that they have no known competing financial interests or personal relationships that could have appeared to influence the work reported in this paper.

Acknowledgements

This study was financed by the Principality of Asturias Regional Government through the project (SV-PA-19-06). The authors gratefully acknowledge the Scientific-Technical Services of the University of Oviedo for chemical and SEM analysis.

Appendix A. Supporting information

Supplementary data associated with this article can be found in the online version at doi:10.1016/j.jece.2021.106794.

References

[1] M. Amodio, S. Catino, P.R. Dambruoso, G. De Gennaro, A. Di Gilio, P. Giungato, E. Laiola, A. Marzocca, A. Mazzone, A. Sardaro, M. Tutino, Atmospheric deposition: sampling procedures, analytical methods, and main recent findings from the scientific literature, Adv. Meteorol. 2014 (2014) 1–27, https://doi.org/10.1155/2014/161730, 161730.

[2] ATSRD (Agency for Toxic Substances and Disease Registry) 2004. Public Health Statement. Strontium. https://www.atsdr.cdc.gov/ToxProfiles/tp159-c1-b.pdf (accessed on 26th July 2021).

[3] Briffa, J., Sinagra, E., Blundell, R. 2020. Heavy metal pollution in the environment and their toxicological effects on humans. Heliyon 6, 1–26. https://doi.org/10.1016/j.heliyon.2020.e04691.

[4] H. Cheng, J. He, X. Zou, J. Li, C. Liu, B. Liu, C. Zhang, Y. Wu, L. Kan, Characteristics of particle size for creeping and saltating sand grains in aeolian transport, Sedimentology 62 (5) (2015) 1497–1511, https://doi.org/10.1111/sed.12191.

[5] De Miguel, E., Iribarren, I., Chacón, E., Ordoñez, A., Charlesworth, S., 2007. Risk-based evaluation of the exposure of children to trace elements in playgrounds in Madrid (Spain). Chemosphere 66, 505–513. https://doi.org/10.1016/j.chemosphere.2006.05.065.

[6] Y. Du, B. Gao, H. Zhou, X. Ju, H. Hao, S. Yin, Health risk assessment of heavy metals in road dusts in urban parks of Beijing, China, Procedia Environ. Sci. 18 (2013) 299–309, https://doi.org/10.1016/j.proenv.2013.04.039.

[7] EEA, Air quality in Europe – 2020 report. No 9/2020. European Environment Agency, Publications Office of the European Union, 2020, https://doi.org/10.2800/786656.

[8] G. Genchi, A. Carocci, G. Lauria, M.S. Sinicropi, A. Catalano, Nickel: Human Health and Environmental Toxicology, Int J. Environ. Res Public Health 17 (3) (2020) 679, https://doi.org/10.3390/ijerph17030679.

[9] G.B. Gerber, A. Léonard, Ph Hantson, Carcinogenicity, mutagenicity and teratogenicity of manganese compounds, Crit. Rev. Oncol. Hemat 42 (2002) 25–34, https://doi.org/10.1016/S1040-8428(01)00178-0.

[10] M. He, X. Wang, F. Wu, Z. Fu, Antimony pollution in China, Sci. Total Environ. 421–422 (2012) 41–50, https://doi.org/10.1016/j.scitotenv.2011.06.009.

[11] W.C. Hinds. Aerosol Technology: Properties, Behavior, and Measurement of Airborne Particles, 2nd ed., John Wiley & Sons, INC., New York, 1999.

[12] D. Hleis, I. Fernández-Olmo, F. Ledoux, A. Kfoury, L. Courcot, T. Desmonts, D. Courcot, Chemical profile identification of fugitive and confined particle emissions from an integrated iron and steelmaking plant, J. Hazard Mater. 250–251 (2013) 246–255, https://doi.org/10.1016/j.jhazmat.2013.01.080.

[13] J. Huang, Q. Liu, X. Guo, Short-term effects of particulate air pollution on human health. Encyclopedia of Environmental Health, Second edition.,, 2019, pp. 655–662, https://doi.org/10.1016/B978-0-12-409548-9.10991-1.

[14] IARC, 2012. Arsenic, Metals, Fibres, and Dusts. IARC Monographs on the Evaluation of Carcinogenic Risks to Humans Volume 100C. ⟨https://publications.iarc.fr/Book-And-Report-Series/Iarc-Monographs-On-The-Identification-Of-Carcinogenic-Hazards-To-Humans/Arsenic-Metals-Fibres-And-Dusts-2012#!⟩ (accessed on 6th July 2021).

[15] IARC, Monographs on the Evaluation of Carcinogenic Risks to Humans. Outdoor air pollution, World Health Organization, 2016 (accessed on 6th July 2021), ⟨https://publications.iarc.fr/538⟩.

[16] IARC, Agents Classified by the IARC Monographs, Volumes 1-128. Last Update: 2 February 2021. IARC Monographs on the Evaluation of Carcinogenic Risks to Humans. International Agency for Research on Cancer, World Health Organization, France, 2021. ⟨https://monographs.iarc.who.int/list-of-classifications⟩ (accessed on 20th April 2021).

[17] IDEPA, 2021. ⟨www.idepa.es/conocimiento/asturias-en-cifras/demografia⟩ (accessed on 28th June 2021).

[18] IGME, 2021. Geological and Mining Institute of Spain. ⟨http://info.igme.es/⟩ (accessed on 2nd July 2021).

[19] M. Kawahara, K. Konoha, T. Nagata, Y. Sadakane, Aluminum and human health: its intake, bioavailability and neurotoxicity, Biomed. Res. Trace Elem. 18–3 (2007) 211–220, https://doi.org/10.11299/brte.18.211.

[20] N.J. Kennedy, W.C. Hinds, Inhalability of large solid particles, J. Aerosol Sci. 33 (2) (2002) 237–255, https://doi.org/10.1016/S0021-8502(01)00168-9.

[21] K.-H. Kim, Z.-H. Shon, P.T. Mauulida, S.-K. Song, Long-term monitoring of airborne nickel (Ni) pollution in association with some potential source processes in the urban environment, Chemosphere 111 (2014) 312–319, https://doi.org/10.1016/j.chemosphere.2014.03.138.

[22] J. Li, B.H. Zheng, Y. He, Y. Zhou, X. Chen, S. Ruan, Y. Yang, C. Dai, L. Tang, Antimony contamination, consequences and removal techniques: a review, Ecotox Environ. Safe 156 (2018) 125–134, https://doi.org/10.1016/j.ecoenv.2018.03.024.

[23] X. Lu, X. Zhang, L.Y. Li, H. Chen, Assessment of metals pollution and health risk in dust from nursery schools in Xi'an, China, Environ. Res. 128 (2014) 27–34, https://doi.org/10.1016/j.envres.2013.11.007.

[24] R.G. Lucchini, M. Aschner, Y. Kim, M. Šarić, Chapter 45 – Manganese. Handbook on the Toxicology of Metals, 4th ed., Volume II, 2015, pp. 975–1011, https://doi.org/10.1016/B978-0-444-59453-2.00045-7.

[25] M. Manousakas, E. Diapouli, C.A. Belis, V. Vasilatou, M. Gini, F. Lucarelli, X. Querol, K. Eleftheriadis, Quantitative assessment of the variability in chemical profiles from source apportionment analysis of PM10 and PM2.5 at different sites within a large metropolitan area, Environ. Res. 192 (2021), 110257, https://doi.org/10.1016/j.envres.2020.110257.

[26] L. Megido, L. Negral, L. Castrillón, Y. Fernández-Nava, B. Suárez-Peña, E. Marañón, Impact of secondary inorganic aerosol and road traffic at a suburban air quality monitoring station, J. Environ. Manag. 189 (2017) 36–45, https://doi.org/10.1016/j.jenvman.2016.12.032.

[27] L. Megido, L. Negral, L. Castrillón, B. Suárez-Peña, Y. Fernández-Nava, E. Marañón, Enrichment factors to assess the anthropogenic influence on PM10 in Gijón (Spain), Environ. Sci. Pollut. R. 24 (2016) 711–724, https://doi.org/10.1007/s11356-016-7858-8.

[28] L. Megido, B. Suárez-Peña, L. Negral, L. Castrillón, S. Suárez, Y. Fernández-Nava, E. Marañón, Relationship between physico-chemical characteristics and potential toxicity of PM10, Chemosphere 162 (2016) 73–79, https://doi.org/10.1016/j.chemosphere.2016.07.067.

[29] J. Mohmand, S.A.M.A.S. Eqani, M. Fasola, A. Alamdar, I. Mustafa, N. Ali, L. Liu, S. Peng, H. Shen, Human exposure to toxic metals via contaminated dust: Bio-accumulation trends and their potential risk estimation, Chemosphere 132 (2015) 142–151, https://doi.org/10.1016/j.chemosphere.2015.03.004.

[30] T. Moreno, T.P. Jones, R.J. Richards, Characterisation of aerosol particulate matter from urban and industrial environments: examples from Cardiff and Port Talbot, South Wales, UK, Sci. Total Environ. 334–335 (2004) 337–346, https://doi.org/10.1016/j.scitotenv.2004.04.074.

[31] L. Negral, B. Suárez-Peña, A. Amado, L. Megido, R. Lara, E. Marañón, L. Castrillón, Settleable matter in a highly industrialized area: Chemistry and health risk assessment, Chemosphere 274 (2021), 129751, https://doi.org/10.1016/j.chemosphere.2021.129751.

[32] L. Negral, B. Suárez-Peña, E. Zapico, Y. Fernández-Nava, L. Megido, J. Moreno, E. Marañón, L. Castrillón, Anthropogenic and meteorological influences on PM10 metal/semi-metal concentrations: Implications for human health, Chemosphere 243 (2020), 125347, https://doi.org/10.1016/j.chemosphere.2019.125347.

[33] M. Oliveira, K. Slezakova, C. Delerue-Matos, M.C. Pereira, S. Morais, Children environmental exposure to particulate matter and polycyclic aromatic hydrocarbons and biomonitoring in school environments: a review on indoor and outdoor exposure levels, major sources and health impacts, Environ. Int. 124 (2019) 180–204, https://doi.org/10.1016/j.envint.2018.12.052.

[34] P. Ponka, J. Tenenbein, W. Eaton, Chapter 41 Iron. Handbook on the Toxicology of Metals, Fourth edition.,, Volume II, 2015, pp. 879–902, https://doi.org/10.1016/B978-0-444-59453-2.00041-X.

[35] N. Rani, B.S. Sastry, K. Dey, Assessment of metal contamination and the associated human health risk from dustfall deposition: a study in a mid-sized town in India, Environ. Sci. Pollut. R. 26 (2019) 23173–23191, https://doi.org/10.1007/s11356-019-05539-7.

[36] O. Rezaei Raja, S. Sobhanardakani, M. Cheraghi, Health risk assessment of citrus contaminated with heavy metals in Hamedan city, potential risk of Al and Cu, Environ. Health Eng. Manag. J. 3 (2016) 131–135, https://doi.org/10.15171/EHEM.2016.11.

[37] J.M. Santos, N.C. Reis, E.S. Galvão, A. Silveira, E.V. Goulart, A.T. Lima, Source apportionment of settleable particles in an impacted urban and industrialized region in Brazil, Environ. Sci. Pollut. R. 24 (2017) 22026–22039, https://doi.org/10.1007/s11356-017-9677-y.

[38] G.A. Sehmel, Particle resuspension: a review, Environ. Int. 4 (1980) 107–127, https://doi.org/10.1016/0160-4120(80)90005-7.

[39] S. Sobhanardakani, Potential health risk assessment of heavy metals via consumption of caviar of Persian sturgeon, Mar. Pollut. Bull. 123 (2017) 34–38, https://doi.org/10.1016/j.marpolbul.2017.09.033.

[40] S. Sobhanardakani, Human health risk assessment of potentially toxic heavy metals in the atmospheric dust of city of Hamedan, west of Iran, Environ. Sci. Pollut. R. 25 (2018) 28086–28093, https://doi.org/10.1007/s11356-018-2818-0.

[41] S. Sobhanardakani, L. Tayebi, S.V. Hosseini, Health risk assessment of arsenic and heavy metals (Cd, Cu, Co, Pb, and Sn) through consumption of caviar of *Acipenser persicus* from Southern Caspian Sea, Environ. Sci. Pollut. R. 25 (2017) 2664–2671, https://doi.org/10.1007/s11356-017-0705-8.

[42] S. Sobhanardakani, Ecological and human health risk assessment of heavy metal content of atmospheric dry deposition, a case study: Kermanshah, Iran, Biol. Trace Elem. Res. 187 (2019) 602–610, https://doi.org/10.1007/s12011-018-1383-1.
[43] C.A. Tylenda, D.W. Sullivan, B.A. Fowler, Chapter 27 – Antimony. Handbook on the Toxicology of Metals, 4th ed., Volume II, 2015, pp. 565–579, https://doi.org/10.1016/B978-0-444-59453-2.00027-5.
[44] USEPA 1989. Risk Assessment Guidance for Superfund, vol. I: Human Health Evaluation Manual. EPA/540/1–89/002. Office of Solid Waste and Emergency Response. US Environmental Protection Agency. Washington, D.C. ⟨https://www.epa.gov/risk/risk-assessment-guidance-superfund-volume-i-human-health-evaluation-manual-supplemental⟩ (accessed on 26th July 2021).
[45] USEPA 1991. Risk Assessment Guidance for Superfund. Volume I — Human Health Evaluation Manual (Part B, Development of Risk-based Preliminary Remediation Goals) EPA/540/R-92/003. Office of Research and Development, Washington, DC 20460. ⟨https://www.epa.gov/risk/risk-assessment-guidance-superfund-rags-part-b⟩ (accessed on 26th July 2021).
[46] USEPA 1996. Soil Screening Guidance: Technical Background Document. EPA/540/R-95/128. Office of Solid Waste and Emergency Response. US Environmental Protection Agency. Washington, DC. Available from: ⟨https://www.epa.gov/superfund/superfund-soil-screening-guidance⟩ (accessed on 26th July 2021).
[47] USEPA 1997. Exposure Factors Handbook – General Factors. EPA/600/P-95/002Fa, vol. I. Office of Research and Development. National Center for Environmental Assessment. US Environmental Protection Agency. Washington, DC. Available from: ⟨https://www.epa.gov/expobox/epa-expobox-and-exposure-factors⟩ (accessed on 26th July 2021).
[48] USEPA 2004. Risk Assessment Guidance for Superfund Volume I: Human Health Evaluation Manual (Part E, Supplemental Guidance for Dermal Risk Assessment) Final. Office of Superfund Remediation and Technology Innovation U.S. Environmental Protection Agency Washington, DC ⟨https://www.epa.gov/risk/risk-assessment-guidance-superfund-rags-part-e⟩ (accessed on 26th July 2021).
[49] USEPA 2014. Human Health Evaluation Manual, Supplemental Guidance: Update of Standard Default Exposure Factors. ⟨https://www.epa.gov/risk/update-standard-default-exposure-factors⟩ (accessed on 26th July 2021).
[50] USEPA 2020. Regional Screening Levels (RSLs) - Generic Tables. ⟨https://www.epa.gov/risk/regional-screening-levels-rsls-generic-tables⟩ (accessed on 26th July 2021).
[51] Y. Wang, M. Qiao, Y. Liu, Y. Zhu, Health risk assessment of heavy metals in soils and vegetables from wastewater irrigated area, Beijing-Tianjin city cluster, China, J. Environ. Sci. 24 (4) (2012) 690–698, https://doi.org/10.1016/S1001-0742(11)60833-4.
[52] A.L. Wani, A. Ara, J.A. Usmani, Lead toxicity: a review, Interdiscip. Toxicol. 8 (2) (2015) 55–64, https://doi.org/10.1515/intox-2015-0009.
[53] L. Weerasundara, D.N. Magana-Arachchi, A.M. Ziyath, A. Goonetilleke, M. Vithanage, Health risk assessment of heavy metals in atmospheric deposition in a congested city environment in a developing country: Kandy City, Sri Lanka, J. Environ. Manag. 220 (2018) 198–206, https://doi.org/10.1016/j.jenvman.2018.04.036.
[54] WHO, Guidelines for Drinking Water Quality, Recommendations, WHO, Geneva, 1993. ⟨https://www.who.int/publications/i/item/9789241549950⟩.
[55] WHO. Chapter 6.8 Manganese. Air Quality Guidelines, 2nd ed., World Health Organization, 2001 (accessed on 26th July 2021), ⟨https://www.euro.who.int/_data/assets/pdf_file/0003/123078/AQG2ndEd_6_8Manganese.pdf⟩.
[56] WHO 2006. Health risks of heavy metals from long-range transboundary air pollution. Convention Task Force on the Health Aspects of Air Pollution. World Health Organization. Regional Office for Europe & Joint WHO/Convention Task Force on the Health Aspects of Air Pollution. ⟨https://apps.who.int/iris/handle/10665/107872⟩ (accessed on 26th July 2021).
[57] R. Zhang, V.L. Wilson, A. Hou, G. Meng, Source of lead pollution, its influence on public health and the countermeasures, Int. J. Health, Anim. Sci. Food Saf. 2 (1) (2015) 18–31, https://doi.org/10.13130/2283-3927/4785.
[58] X.-H. Zhu, P.-P. Zhang, X.-G. Chen, D.-D. Wu, Y. Ye, Natural and anthropogenic influences on the arsenic geochemistry of lacustrine sediment from a typical fault-controlled highland lake: Yangzonghai Lake, Yunnan, China, Environ. Earth Sci. 75 (2016) 217, https://doi.org/10.1007/s12665-015-4924-3.